Received: 2 December 2020 | Accepted: 10 March 2021

DOI: 10.1002/ajb2.1713

RESEARCH ARTICLE

American Journal of Botany

Early Cretaceous abietoid Pinaceae from Mongolia and the history of seed scale shedding

Fabiany Herrera[1] | Gongle Shi[2] | Maya A. Bickner[1] | Niiden Ichinnorov[3] | Andrew B. Leslie[4] | Peter R. Crane[5,6] | Patrick S. Herendeen[1]

[1]Chicago Botanic Garden, Glencoe, Illinois 60022, USA

[2]State Key Laboratory of Palaeobiology and Stratigraphy, Nanjing Institute of Geology and Palaeontology and Center for Excellence in Life and Paleoenvironment, Chinese Academy of Sciences, Nanjing 210008, China

[3]Institute of Paleontology, Mongolian Academy of Sciences, Ulaanbaatar–15160, Mongolia

[4]Department of Geological Sciences, Stanford University, California 94305, USA

[5]Oak Spring Garden Foundation, Oak Spring, Upperville, Virginia 20184, USA

[6]Yale School of the Environment, Yale University, New Haven, Connecticut 06511, USA

Correspondence

Fabiany Herrera, Chicago Botanic Garden, Glencoe, Illinois 60022, USA.
Email: fherrera@chicagobotanic.org

Abstract

Premise: Seed cones of extant Pinaceae exhibit two mechanisms of seed release. In "flexers" the cone scales remain attached to the central axis, while flexing and separating from each other to release the seeds. In "shedders" scales are shed from the axis, with the seeds either remaining attached to the scale or becoming detached. The early fossil history of Pinaceae from the Jurassic to Early Cretaceous is dominated by flexing seed cones, while the systematic information provided by shedding fossil cones has been overlooked and rarely integrated with data based on compression and permineralized specimens. We describe the earliest and best-documented evidence of a "shedder" seed cone from the Aptian–Albian of Mongolia.

Methods: Lignite samples from Tevshiin Govi locality were disaggregated in water, washed, and dried in air. Fossils were compared to material of extant Pinaceae using LM and CT scans.

Results: *Lepidocasus mellonae* gen. et sp. nov. is characterized by a seed cone that disarticulated at maturity and shed obovate bract–scale complexes that have a distinctive ribbed surface and an abaxial surface covered with abundant trichomes. The ovuliferous scale has ca. 30–40 resin canals, but only scarce xylem near the attachment to the cone axis. Resin vesicles are present in the seed integument. Phylogenetic analysis places *Lepidocasus* as sister to extant *Cedrus* within the abietoid grade.

Conclusions: The exquisite preservation of the trichomes in *L. mellonae* raises questions about their potential ecological function in the cones of fossil and living Pinaceae. *Lepidocasus mellonae* also shows that a shedding dispersal syndrome, a feature that has often been overlooked, evolved early in the history of Pinaceae during the Early Cretaceous.

KEYWORDS

anatomy, *Cedrus*, cone scale, Cretaceous, Jurassic, *Pityolepis*, seed dispersal, trichomes

The Pinaceae are the most diverse group of living conifers, with 231 species (Farjon, 2010). Most of the 11 living genera are species-poor and are placed in two major groups (Leslie et al., 2012; Gernandt et al., 2018): the abietoids with *Cedrus* (3 spp.), *Tsuga* (9 spp.), *Nothotsuga* (1 sp.), *Pseudolarix* (1 sp.), *Keteleeria* (3 spp.), and *Abies* (47 spp.), and the pinoids with *Larix* (11 spp.), *Pseudotsuga* (4 spp.), *Picea* (38 spp.), *Cathaya* (1 sp.), and *Pinus* (113 spp.). The split between crown abietoids and pinoids is estimated to have occurred in the Late Triassic or Early Jurassic (ca. 206–188 mya) (Leslie et al., 2018; Ran et al., 2018), significantly before the earliest well-documented fossil evidence of the family from the Late Jurassic (Rothwell et al., 2012). Nevertheless, fossils of probable stem group Pinaceae are known from the Triassic and Early Jurassic based on seed cones of *Schizolepidopsis* (see Zhang et al., 2011; Leslie et al., 2013; Domogatskaya and Herman, 2019; Matsunaga et al., 2021), and there are other putative pinaceous fossils of Jurassic age that have been assigned to several different genera: *Pityolepis* for cone scales, *Pityospermum* for winged seeds, *Pityocladus* for vegetative shoots, and *Pityophyllum* for detached leaves (Seward, 1919). Many of these isolated, early, potentially pinaceous fossils are based only on compressions/impressions, making it hard to evaluate their relationships.

The obscure Jurassic history of Pinaceae contrasts markedly with its diverse and abundant Early Cretaceous fossil record, which documents remarkable morphological

diversity, including the seed cone genera *Pseudoaraucaria* (Alvin, 1957a, 1957b, 1960, 1988; Miller and Robison, 1975), *Obirastrobus* (Ohsawa and Nishida, 1992), and especially *Pityostrobus*, a likely polyphyletic genus that includes ≥30 species (e.g., Herrera et al., 2016; Smith et al., 2016). Recent phylogenetic hypotheses suggest that several Early Cretaceous *Pityostrobus* species may belong to stem lineages of extant abietoids and pinoids (Smith et al., 2016; Gernandt et al., 2018).

A feature that has been overlooked in studies of Pinaceae but that may be relevant to understanding the early evolutionary history of the group is the mode of seed dispersal. Losada et al. (2018) found a set of anatomical features that help to explain the mechanism for the disarticulation of the seed cones in several genera of Pinaceae. In cones of "shedders," including those of the genera *Abies*, *Cedrus*, *Keteleeria*, and *Pseudolarix*, there is only a small amount of xylem, composed of thin-walled tracheids with wide lumens and high hydraulic efficiency, near the base of the cone scales. Bract–scale complexes are easily shed from the cone axis and release the winged seeds at maturity (Losada et al., 2018). In addition, *Abies* and *Cedrus* appear to have a consistent area at the base of the scale where abscission occurs, while *Keteleeria* and *Pseudolarix* do not (J. M. Losada, Instituto de Hortofruticultura Subtropical y Mediterranea, personal observation). In "flexers," which include all pinoids plus *Tsuga* and *Nothotsuga*, the proximal portion of the cone scale xylem is well developed, tough, and relatively poorly conductive (Losada et al., 2018). Shedding seed cones occur in about a quarter of living Pinaceae species, and the phylogenetic distribution of this feature suggests that it may have been important during the early diversification and expansion of the group.

In this paper, we present new fossils from the Early Cretaceous of Mongolia that provide the earliest and best-documented evidence of seed cone scale shedding in Pinaceae, based on hundreds of well-preserved isolated bract–scale complexes that also show morphological and anatomical evidence of programmed disarticulation. The presence of clear shedding behavior in the early fossil history of Pinaceae raises questions about the recognition of shedders in the Mesozoic record and the importance of shedding in the evolution of the family.

MATERIALS AND METHODS

The fossils reported in this study were collected at the Tevshiin Govi lignite open cast mine in central Mongolia. The fossil-bearing rocks belong to the Tevshiingovi Formation, considered to be Aptian–Albian in age (125–100.5 mya) based on stratigraphic correlations (Graham et al., 2001; Hasegawa et al., 2018) and palynomorphs recovered from the plant localities (Ichinnorov, 2003; Nichols et al., 2006; Ichinnorov et al., 2012). The lignites at Tevshiin Govi contain little inorganic sediment, and their deposition appears to have been largely autochthonous, under peat swamp conditions (Leslie et al., 2013; Herrera et al., 2015; Shi et al., 2016).

The fossils occur in two unconsolidated lignites collected at roughly the same stratigraphic level, and only ~11 m apart, in the summer of 2019 (sample PSH445, 45°58′51.6″N, 106°07′09.5″E; and sample PSH417, 45°58′51.7″N, 106°07′09.0″E). Most of the specimens were recovered from PSH445.

The samples were disaggregated in soap and hot water followed by dilute hydrogen peroxide (3%). Organic material was separated from the resulting slurry by gentle sieving and panning over 125–500 µm mesh sieves. The fossil material was then air dried, and selected mesofossils were cleaned with hydrochloric and hydrofluoric acids, washed thoroughly, and air dried. Fossils were photographed (LM) at the Chicago Botanic Garden (CBG) using a Canon Rebel (Tokyo, Japan) camera with 100 mm macrolens attached to a Stackshot system (Traverse City, Michigan, USA), and digital images were merged using Helicon Focus software (Kharkiv, Ukraine).

Fossils selected for anatomical sectioning were soaked in 10% hydrochloric acid (for ~7 d), followed by Aerosol OT (10% solution of sodium dioctyl sulfosuccinate in alcohol for ~30 d), and then taken through an ethanol series (70% to absolute ethanol; ~2 d) before embedding in Technovit 7100 following the prescribed protocol (https://www.kulzer-technik.com/). Transverse and longitudinal sections, ca. 4–7 µm thick, were made of the embedded material using a Leica 2030 microtome (Wetzlar, Germany). Slides were mounted in Hydromount no. 17966 (Hatfield, Pennsylvania, USA). Cuticles were obtained by macerating bract–scale complexes using dilute household bleach (~1% sodium hypochlorite solution) or dilute hydrogen peroxide. The pieces of cuticle were mounted on slides with Eukitt (Hatfield, Pennsylvania, USA). Fossils selected for maceration were soaked in dilute hydrogen peroxide for ~2 d. Anatomical slides and cuticles were examined with differential interference contrast (DIC) and fluorescence microscopy illumination using a Leica DMLB microscope. Slides were photographed with a Jenoptik Gryphax (Jena, Germany) digital camera at GBC (Field Museum).

The holotype, as well as cone scales of extant Pinaceae, were examined using a General Electric dual tube X-ray computed tomography scanner (Boston, Massachusetts, USA) in the Department of Organismal Biology and Anatomy at the University of Chicago. The specimens were scanned at 50 kV for 37 min, with a voxel size 10 µm. The data sets were processed using Avizo Lite 2020.2 (Waltham, Massachusetts, USA) to obtain successive virtual sections, translucent volumes, and surface renderings. Appendixes S1, S2, and S3 include the videos of CT scan data sets and volume renderings of the holotype. Measurements (length, width, area calculations, etc.) of the bract–scale complexes were obtained with ImageJ 1.52 v.

Extant material from CBG living collections was examined for comparison. Fossil material described in this study is housed in the paleobotanical collections of the Field Museum, Chicago, Illinois, USA (FMNH: collection numbers with the prefix PP), and in the Institute of Paleontology in Ulaanbaatar, Mongolia (Mongolian Paleontological Center–Flora).

To assess the phylogenetic position of the new fossils, we used the morphological matrix for living and fossil Pinaceae from Gernandt et al. (2018). This matrix includes plastid DNA data and morphological characters. A small number of states and scorings (characters 68, 77, 83) were modified from the list of definitions and matrix presented by Gernandt et al. (2018). We also added an additional morphological character (character 189) to reflect the anatomy of shedding cones based on Losada et al. (2018). *Pinus haboroensis* (based exclusively on leaves) and *Pinus mutoi* were excluded from our analysis on the basis of their unstable positions in the analysis of Gernandt et al. (2018). The modified morphological matrix includes 189 morphological characters and 88 taxa; all changes and the definition of the new character are noted in the matrix. The morphological matrix is available at the MorphoBank website (http://morphobank.org/permalink/?P3725). Parsimony analyses and heuristic searches were carried out with 10,000 replicates of random taxon addition and tree-bisection–reconnection (TBR) branch swapping in the program PAUP* 4.0a (build 168) for Macintosh (X86) (Swofford, 2003). All morphological characters were treated as unordered. Bootstrap analyses were performed on the morphological data using 100 replicates and full heuristic searches. Appendix S4 includes the complete tree recovered from our phylogenetic analysis.

SYSTEMATICS

Order

Coniferales

Family

Pinaceae Lindley
"Abietoid grade"

Genus

Lepidocasus Herrera, Shi, Bickner, Ichinnorov, Leslie, Crane, et Herendeen gen. nov.

Type

Lepidocasus mellonae Herrera, Shi, Bickner, Ichinnorov, Leslie, Crane, et Herendeen sp. nov.

Generic diagnosis

Seed cones disarticulating at maturity into bract–scale complexes that are circular to elliptical (poorly developed) to distinctly obovate (well developed) in outline. Ovuliferous scale subtended by a short bract and bearing two winged seeds on the adaxial surface. Interseminal ridge not extending more than half of seed height. Abaxial and adaxial surfaces of ovuliferous scales strongly ribbed in a fan-like pattern. Ovuliferous scales mostly sclerotic proximally and distally, but with scarce xylem near the base of scale. Bract separation first medially then along lateral margins. Bract glabrous, but abaxial and adaxial surfaces of ovuliferous scales conspicuously tomentose, covered with non-glandular trichomes. Resin vesicles present in seed coat.

Species

Lepidocasus mellonae Herrera, Shi, Bickner, Ichinnorov, Leslie, Crane, et Herendeen sp. nov.

Specific diagnosis

As for the genus, with the following additions. Ovuliferous scales ca. 3.1–16.6 mm long and ca. 3.1–10.3 mm wide. Free part of bract up to ca. 2.4–5.1 mm long and up to ca. 1.0–2.1 mm wide. Base of ovuliferous scales concavo-convex in outline and auricled. Apex of ovuliferous scales rounded to truncate. Four abaxial resin canals enter the base of the bract–scale complex; ca. 30–40 resin canals present near middle to distal portion of the ovuliferous scale. Bract with two resin canals. Trichomes conical, ca. 44–155 μm long and ca. 7–22 μm wide. Small median stomatal band present in free part of bract.

Holotype

PP60450. Figures 1A, B and 5A–F.

Other material

PP60451–PP60500. Figures 1B–D, 2, 3, and 4.

Repository

Paleobotanical Collections, The Field Museum, Chicago, Illinois, USA. Additional material deposited in the Institute of Paleontology in Ulaanbaatar, Mongolia (Mongolian Paleontological Center–Flora).

Stratigraphic position and age

Tevshiingovi Formation, Aptian–Albian stage (125–100.5 mya), Early Cretaceous.

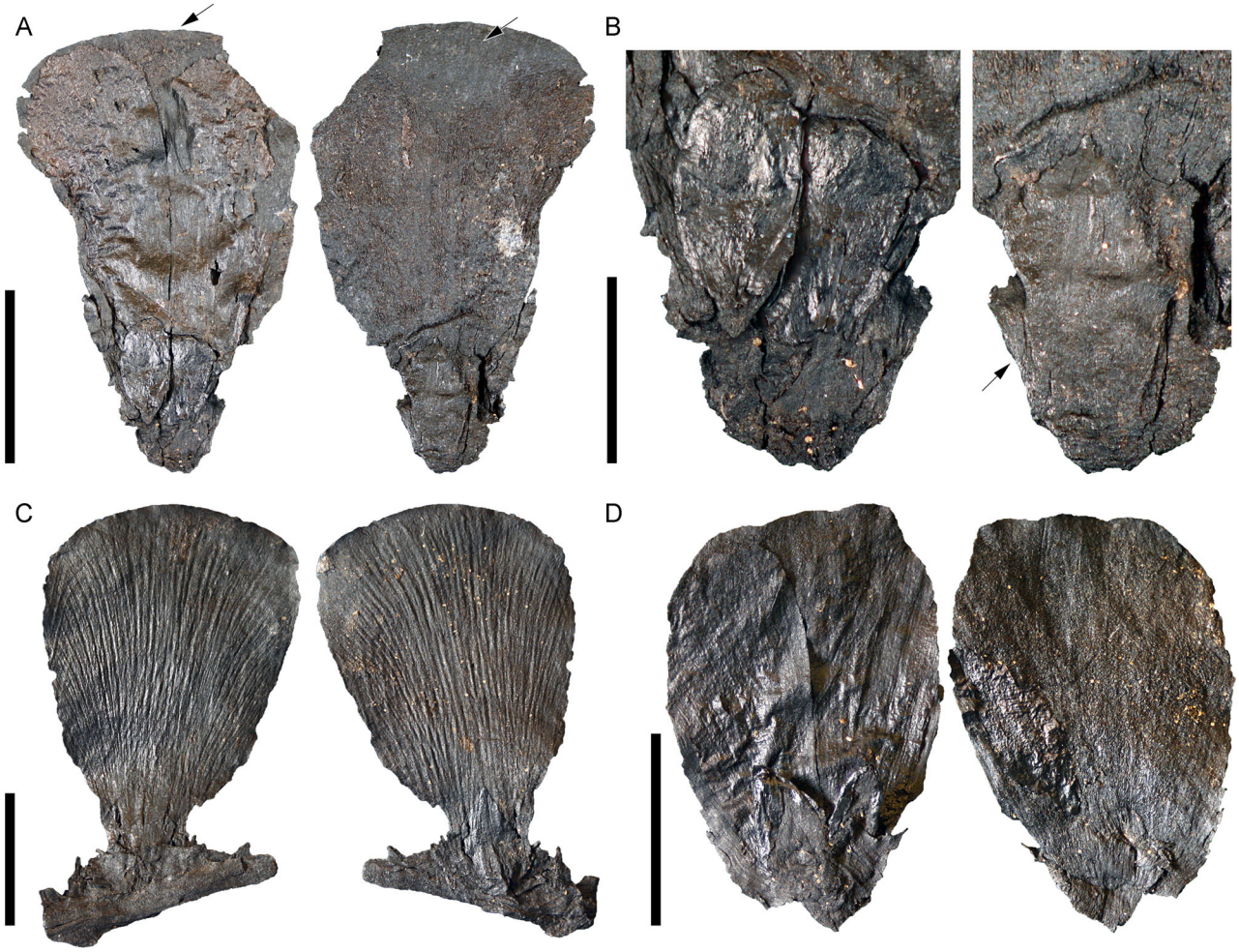

FIGURE 1 *Lepidocasus mellonae* gen. et sp. nov.: light micrographs of mature isolated bract–scale complexes showing adaxial and abaxial surfaces (left and right, respectively). (A) Holotype showing the adaxial surface of the ovuliferous scale with two attached winged seeds and a tomentose distal area (arrow), and the abaxial surface of the ovuliferous scale with bract, tomentose surface proximal and glabrous surface distally (arrow) (PP60450). (B) Detail of bract–scale complex from A, showing two attached winged seeds with their seed bodies covered by wing tissue; note pollen grains (yellow) and glabrous bract (arrow) with a toothed margin and acuminate apex. (C) Bract–scale complex attached to a short section of the cone axis showing the strongly ribbed, tomentose surfaces, and pollen grains (yellow) on the abaxial surface (PP60451). (D) Bract–scale complex lacking the base and bract but showing the adaxial surface with two attached winged seeds and the abaxial surface with prominent ribs, tomentose surface, and abundant pollen grains (yellow) (PP60452). Scale bars = 5 mm (A, C, D); 2 mm (B)

Localities

Tevshiin Govi coal mine (PSH445: 45°58′51.6″N, 106°07′09.5″E, and PSH417: 45°58′51.7″N, 106°07′09.0″E), central Mongolia.

Etymology

From the Greek *lepis* ("scale") and the Latin *casus* ("fall"), referring to the shedding nature of the bract–scale complexes. The species is named in honor of Rachel Lambert "Bunny" Mellon (1910–2004) for her contributions to horticulture and plant science research through the Oak Spring Garden Foundation (https://www.osgf.org/).

Detailed description

Seed cone axis

A single fragmentary cone axis with one attached bract–scale complex has been recovered from the lignite (Figure 1C). The axis fragment is ~8.3 mm long, ~1 mm wide, and bears three additional abscission scars that appear helically arranged. The bract–scale complex is borne at ~71° to the cone axis (Figure 1C).

Bract–scale complex

Approximately 250 isolated bract–scale complexes have been recovered from the Tevshiin Govi lignite. The

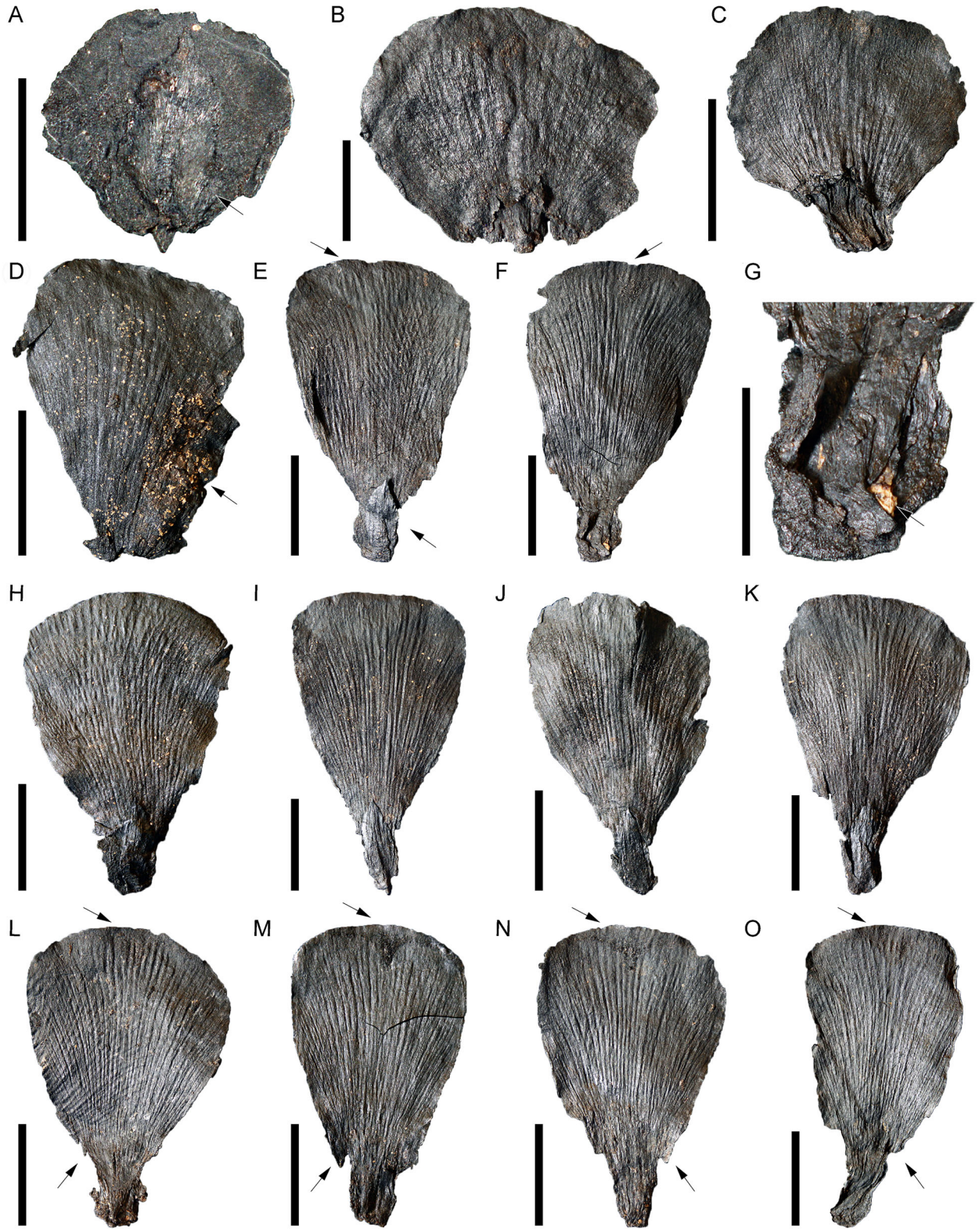

FIGURE 2 *Lepidocasus mellonae* gen. et sp. nov.: light micrographs of isolated bract–scale complexes. (A–C) Small circular to elliptical bract–scale complexes showing the well-developed abaxial bract (A, arrow) and ribbed adaxial surfaces (B, C) (PP60453–PP60455). (D) Abaxial surface of ovuliferous scale showing abundant clumps of pollen grains (yellow; arrow) (PP60456). (E–G) Bract–scale complex showing bract (lower arrow) on the abaxial surface (E), tomentose and glabrous areas (upper arrows respectively) on both surfaces (E, F), and the interseminal ridge and mass of pollen grains (yellow; arrow) at the base of the adaxial surface (G) (PP60457). (H–K) Mature bract–scale complexes in abaxial view showing the obovate ovuliferous scales, ribbed surfaces, and tomentose and glabrous areas (PP60458–PP60461). (L–O) Mature bract–scale complexes in adaxial view, showing the obovate ovuliferous scales, ribbed surfaces, auricles (lower arrows), and tomentose distal areas (upper arrows) (PP60462–PP60465). Scale bars = 5 mm (C–F, H–O); 2 mm (A, B, G)

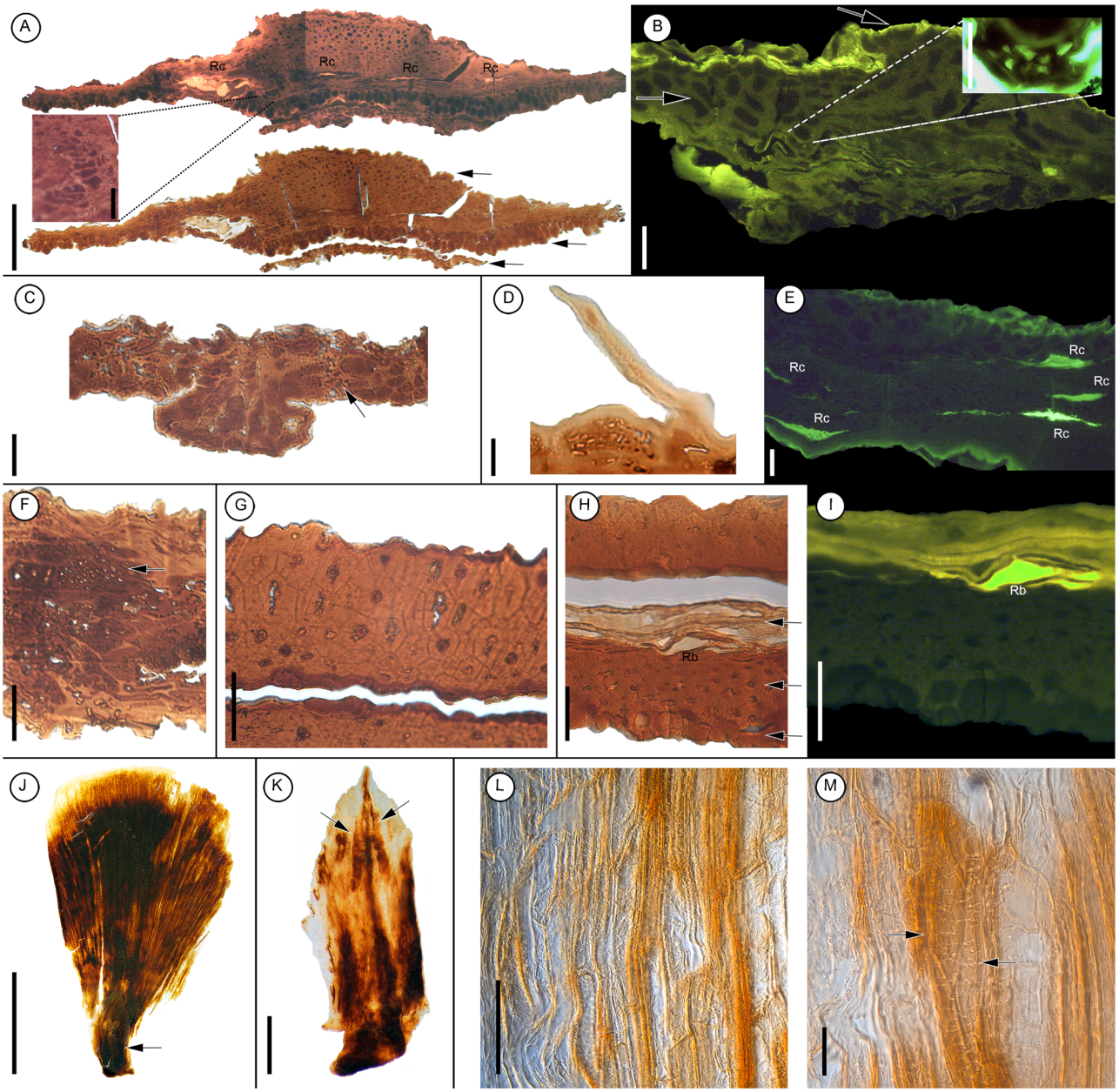

FIGURE 3 *Lepidocasus mellonae* gen. et sp. nov.: light (A, C, D, F–H, J–M) and fluorescence (A, B, E, I) micrographs of anatomy of isolated bract–scale complexes and seeds. (A) Transverse section near the base of the bract–scale complex photographed under fluorescence microscopy blue/green (above) and light (below) showing the bract (lower arrow), the abaxial portion of the ovuliferous scale composed mainly of large parenchyma cells with dark contents (middle arrow), and the adaxial portion and core of the ovuliferous scale composed mainly of sclerenchyma (upper arrow) with four resin canals (Rc); note inset showing detail of a small zone of xylem composed of several tracheids with wide lumens (PP60466). (B) Transverse section near the base of cone scale showing massive sclerenchymatous tissue (left arrow) and small zone of xylem composed of tracheids with wide lumens (inset); thin cuticle indicated by upper arrow (PP60467). (C) Detail of transverse section of bract composed mostly of large parenchyma cells with dark contents and scattered sclerenchyma (arrow) (PP60468). (D) Detail of unicellular trichome in longitudinal section on abaxial surface of ovuliferous scale; note the epidermal cells and thick cuticle (PP60469). (E) Transverse section near the distal end of the ovuliferous scale showing adaxial and abaxial resin canals (Rc) as well as between the vasculature (PP60467). (F) Detail of transverse section near the distal end of the ovuliferous scale showing large zones of xylem (arrow) (PP60469). (G) Detail of transverse section of seed coat showing thick sclerotesta composed of thick-walled stone cells (PP60470). (H) Detail of transverse section of seed showing thin sarcotesta (lower arrow), sclerotesta (middle arrow), and endotesta (upper arrow); note resin body (Rb) (PP60471). (I) Detail from H showing the three tissue layers of the seed and resin body (Rb). (J) Partially macerated bract–scale complex showing longitudinal distribution and abundance of resin canals; note bract (arrow) (PP60472). (K) Isolated partially macerated bract showing two large resin canals distally (arrows) (PP60472). (L) Longitudinal view of partially macerated tracheids of the ovuliferous scale (PP60472). (M) Detail of tracheid with partially preserved alternate biseriate pits (arrows) (PP60472). Scale bars = 5 mm (J); 1 mm (K); 200 μm (A, L); 50 μm (B, C, E–I, M, insets); 10 μm (D)

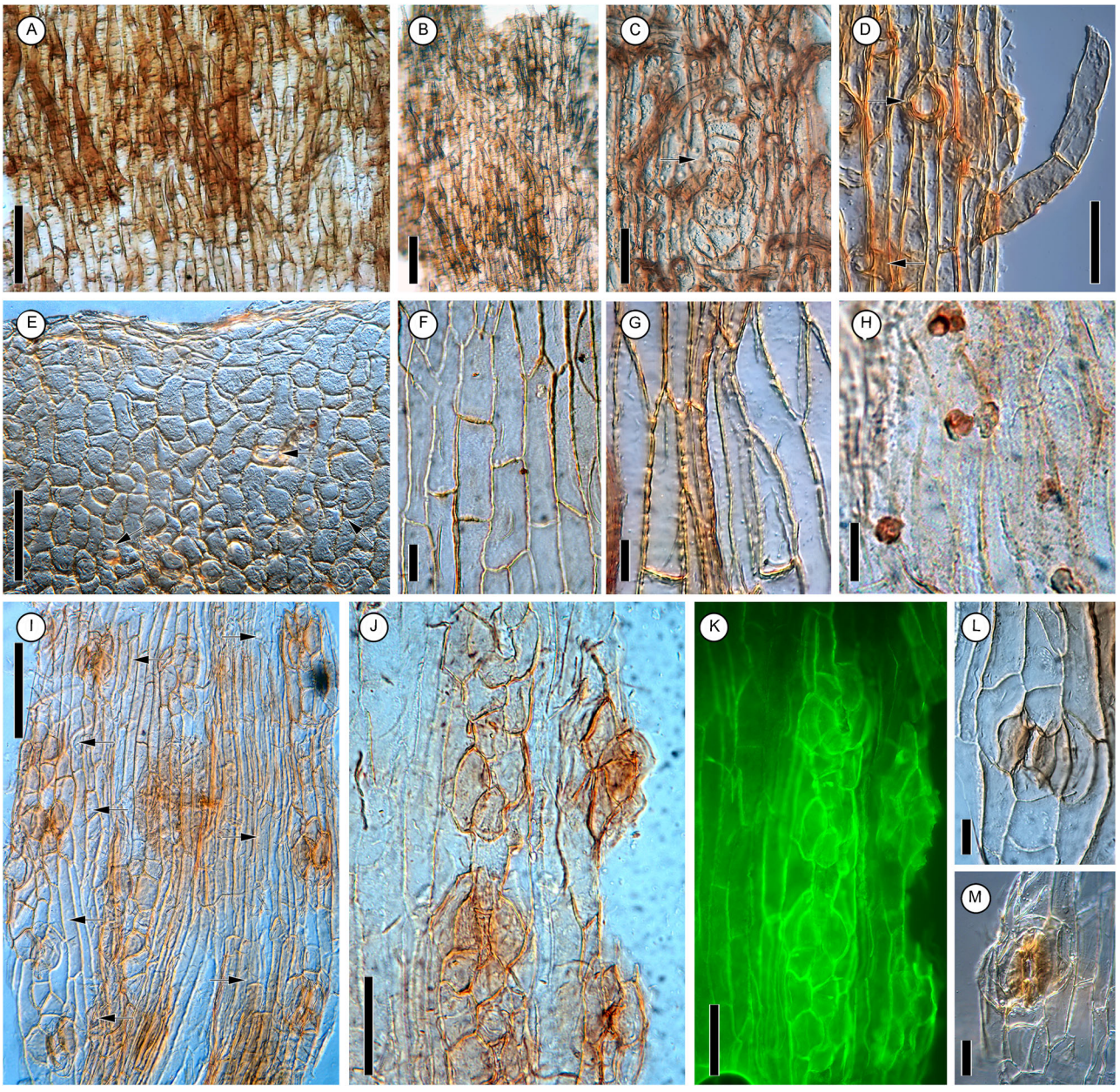

FIGURE 4 *Lepidocasus mellonae* gen. et sp. nov.: light micrographs of abaxial cuticles from ovuliferous scale (A–E) and bract (F–M). (A, B) Outer surface showing abundant trichomes (PP60473). (C) Outer surface showing detail of trichomes and a probable stomatal complex (arrow) (PP60473). (D) Detail of outer surface showing rows of elongate epidermal cells, nearly circular trichome bases (arrows), and bicellular trichome (PP60474). (E) Detail of inner surface showing irregularly arranged polygonal epidermal cells and trichome bases (arrows) from the distal end of ovuliferous scale (PP60475). (F) Detail of outer surface of bract showing seven rows of elongate epidermal cells (PP60476). (G) Detail of inner surface in the distal portion of the bract showing eight rows of epidermal cells (PP60462). (H) Detail of outer surface of bract showing probable papillae (PP60476). (I) Inner surface of bract showing eight widely separated stomatal complexes in two stomatal bands (PP60476). (J) Detail of outer surface showing stomatal band with six, narrowly separated complexes (PP60476). (K) Same from J photographed under fluorescence. (L, M) Detail of outer surface showing stomatal complex with sunken guard cells and eight subsidiary cells that are arranged in two rings (PP60462, PP60476). Scale bars = 100 μm (A, E, I); 50 μm (B–D, J, K); 20 μm (F–H, L, M)

bract–scale complex is papery and consists of an ovuliferous scale subtended by a bract. Ovuliferous scales vary in shape from nearly circular to elliptical or obovate (Figures 1 and 2), ca. 3.1–16.6 mm long (n = 20, SD = 4.09), ca. 3.1–10.3 mm wide, measured at the widest point (n = 20, SD = 1.8), and ca. 0.25–2.25 mm wide measured at the most proximal part of the bract–scale complex (n = 20, SD = 0.5). Nearly circular to elliptical ovuliferous scales are relatively small compared to obovate specimens (Figure 2A–C) (smallest specimen ~3.1 mm long and ~3.1 mm wide vs. largest specimen ~16 mm long and ~10.3 mm wide). Small scales (<5 mm long) are also rare in the lignite, and likely represent an immature or poorly developed stages of growth. Ovuliferous scales are ca.

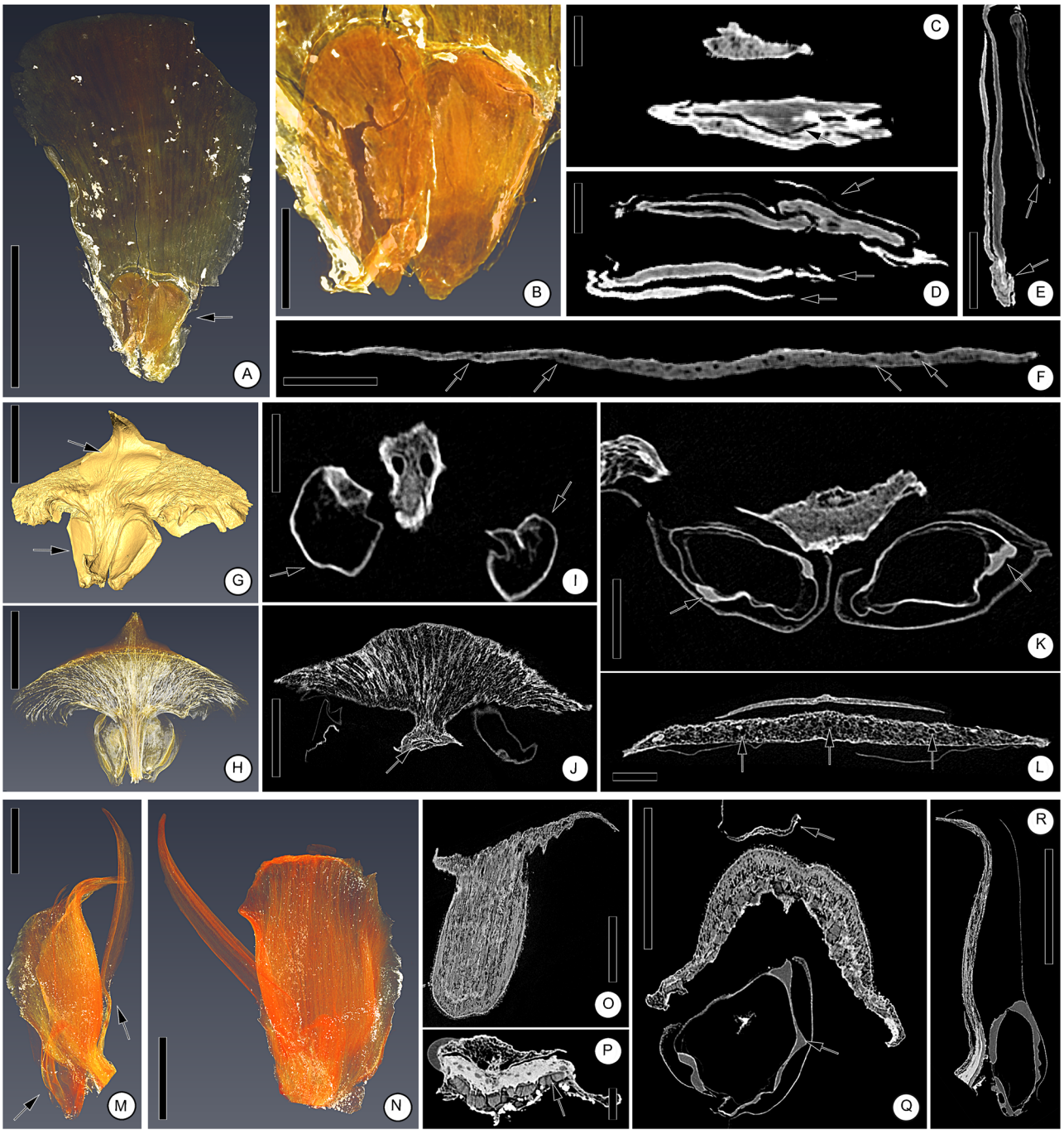

FIGURE 5 Digital micro-CT images of bract–scale complexes of fossil and living Pinaceae. (A–F) *Lepidocasus mellonae* gen. et sp. nov., holotype (PP60450). (A) Translucent volume rendering showing adaxial view with two seeds (arrow) and the ribs of the ovuliferous scale (see Appendix S1). (B) Detail from A showing two seeds with pointed micropyles directed toward the base of the bract–scale complex. (C) Transverse sections near the base of the bract–scale complex, before separation of bract and ovuliferous scale (top) and after their medial separation (bottom, arrow). (D) Transverse section showing separated bract (lower arrow), ovuliferous scale (central arrow), and two winged seeds (upper arrow). (E) Longitudinal section showing seed (upper arrow), bract separated from ovuliferous scale, and interseminal ridge (lower arrow). (F) Transverse section near the tip of the ovuliferous scale showing several resin canals (arrows). (G–L) *Abies koreana* E.H. Wilson. (G) Volume rendering of bract–scale complex in oblique abaxial view showing bract (upper arrow) and two seeds (lower arrow). (H) Translucent volume rendering of G showing abundant resin canals and vascular strands. (I) Transverse section near the base of the bract–scale complex showing two resin canals and two seeds (arrows). (J) Oblique tangential section showing abundant resin canals, vascular strands, and two seeds; note that bract separation occurs first medially (arrow). (K) Transverse section at the level of the seeds showing vesiculate integuments (arrows). (L) Transverse section above the level of the seeds showing bract and numerous resin canals (arrows). (M–R) *Keteleeria davidiana* (Bertrand) Beissn. (M) Translucent volume rendering of bract–scale complex in lateral view showing the bract (upper arrow) and seed (lower arrow). (N) Translucent volume rendering in M in oblique abaxial view showing ribbed ovuliferous scale. (O) Oblique section showing abundant resin canals and vascular strands. (P) Transverse section showing separation of the bract occurring first laterally and resin canals (arrow). (Q) Transverse section showing bract (upper arrow), ovuliferous scale, and vesiculate integument (lower arrow). (R) Longitudinal section showing resin canals and vascular strands in ovuliferous scale; note vesiculate winged seed. Scale bars = 5 mm (A, G, H, J, M–O, Q, R); 1 mm (B, E, F, I, K, L); 500 µm (C, D, P)

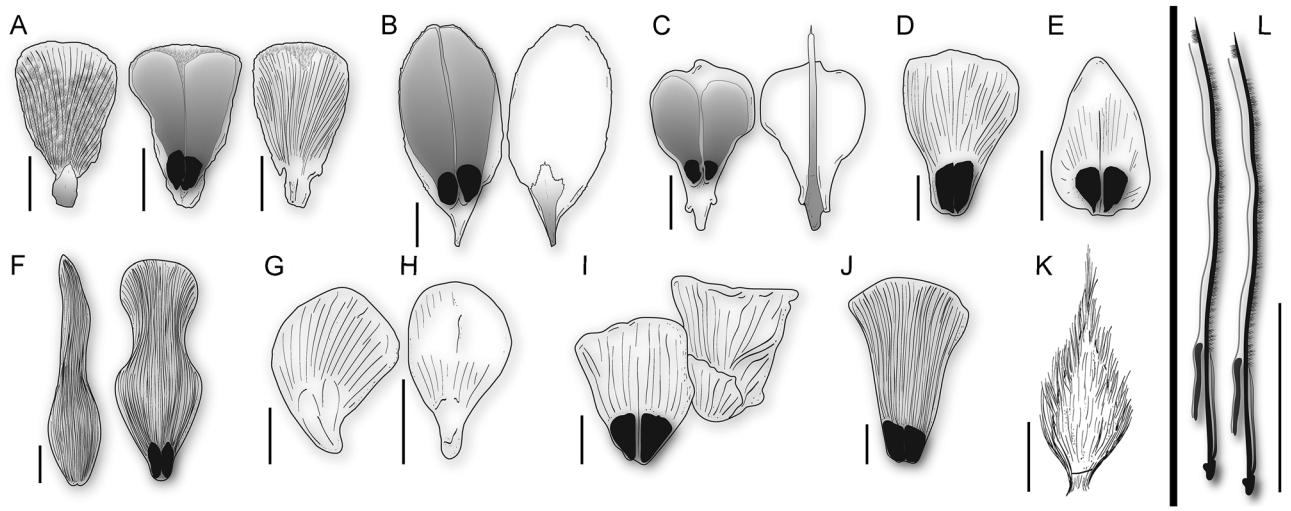

FIGURE 6 Line drawings of selected Early Cretaceous (A–I, K) and Jurassic (J) bract–scale complexes. (A) *Lepidocasus mellonae* gen. et sp. nov., in abaxial (left) and adaxial views (middle with seeds, right without seeds) showing ribbed surfaces and the distribution of trichomes. (B) *Picea farjonii* in adaxial and abaxial views modified after Herrera et al. (2016). (C) *Pityostrobus stockeyae* in adaxial and abaxial views modified after Herrera et al. (2016). (D) *Pityolepis* sp. in adaxial view modified after Krassilov (1982). (E) *Pseudolarix erensis* in adaxial view modified after Krassilov (1982). (F) *Pityolepis tollii* in abaxial and adaxial views modified after Nathorst (1907) and Herman and Spicer (2010). (G) *Pinites* (*Pityolepis*) *tsugaeformis* modified after Nathorst (1897). (H) *Pinites* (*Pityolepis*) *pygmaeus* modified after Nathorst (1897). (I) *Pityolepis rugosa* in adaxial and abaxial views modified after Seward (1927). (J) *Pityolepis sphenoides* in adaxial view modified after Zheng et al. (2001). (K) *Pityolepis crassa* modified after Prynada (1962). (L) Diagram of trichome distribution on abaxial and adaxial surfaces of *L. mellonae* gen. et sp. nov. Scale bars = 1 cm (F); 5 mm (A–E, G–L)

200–500 μm thick proximally and become thinner, ca. 100–150 μm distally. The abaxial and adaxial surfaces of ovuliferous scales are strongly ribbed from proximal to distal ends. Ribs are longitudinally oriented in a fan-like pattern and form tight bands of ridges (ca. 30–45) and furrows (Figures 1, 2, 3J, 5A, and 6A).

The ovuliferous scale base is concavo-convex in outline and auricled (i.e., ear-like projection originated near the scale base) (Figures 1C and 2L–O). The apex of the ovuliferous scales is rounded to approximately truncate in outline (Figures 1A, C and 2A–F, H–O). Scale margins are more or less undulate in appearance and have toothed and untoothed areas in the same specimen. When toothed, the ovuliferous scales have fine, irregularly spaced, spine-like teeth (ca. 230–765 μm long, n = 10, SD = 200). The apices of the minute teeth may be directed either distally or proximally (Figures 1C and 2H–O).

Ovuliferous scales are mostly sclerotic proximally and distally (Figure 3A, B, E). Below the level of the seeds, there is a clear division between the hypodermal abaxial and adaxial zones. Abaxially, the hypodermal tissue is thin (ca. 30–90 μm thick), mainly parenchymatous (individual cells ca. 15–40 μm in diameter), and filled with dark contents (Figure 3A). Adaxially, the scale is dominantly sclerotic (ca. 20–255 μm thick) with individual cells ca. 5–33 μm in diameter. The xylem area appears extremely limited and is surrounded by sclerenchyma tissue near the proximal end of the scale (Figure 3A, B); tracheids are relatively large in transverse section (ca. 5–60 μm, measured at the longest axis) and show thin walls (Figure 3A, B). Partially macerated ovuliferous scales (Figure 3L) show tracheids in longitudinal view (ca. 310–620 μm long and ca. 50–105 μm wide), with poorly preserved, biseriate, alternately arranged pitting (ca. 16–20 μm in diameter) (Figure 3M).

Resin canals, best seen under fluorescence, are ca. 65–175 μm wide and appear highly compressed (Figure 3A, E and 5F). Four abaxial resin canals enter the base of each bract–scale complex and immediately branch upward to become both abaxial and adaxial at the level of the seeds. Distally, the resin canals undergo additional multiple divisions and are found abaxially, adaxially, and between the vasculature tissue (Figure 3E, J). At least 30–40 resin canals are observed from the middle part to the distal end of the ovuliferous scale.

The bract is fused to the abaxial surface of the scale proximally but is free distally, and its separation from the ovuliferous scale occurs first medially, then along its lateral margins (Figures 1B [right] and 5C–E). The bract is thin (ca. 40–250 μm thick) and is shorter than the ovuliferous scale or, only occasionally, in very small bract–scale complexes, about the same length as the scale (Figures 2A and 3K).

The free part of the bract is up to ca. 2.4–5.1 mm long (n = 10, SD = 0.8) and up to ca. 1.0–2.1 mm wide (n = 10, SD = 0.3). In large bract–scale complexes (i.e., >10 mm long) the free part of the bract is approximately one-fifth of the scale length. In large and small bract–scale complexes the bract is roughly elliptical to ovate in outline, with teeth of varying sizes that are irregularly spaced along the margin (Figures 1A–C [right]; 2A, E, H–K; and 3K). The bract apex is consistently acuminate, ending in a small acute tip (Figures 1B [right], 2A, and 3K).

Bracts are mostly parenchymatous (individual cells ca. 13–43 μm in diameter) and filled with dark contents, and with small sclerotic areas (individual cells ca. 10–14 μm in diameter) (Figure 3C). Two resin canals (ca. 120–170 μm wide) are observed in the macerated material (Figure 3K).

Trichomes, cuticle, and stomata

The surface of the bract appears glabrous, but the ovuliferous scales are prominently tomentose and bear unicellular or bicellular non-glandular trichomes on both the abaxial and adaxial surfaces in areas that are loosely defined, both positively and negatively, by the position of the winged seeds (Figures 1, 2, 3D, 4A–E, and 6A, L). Adaxially, a roughly Y–shaped small tomentose area (ca. 4.5–7.1 mm^2) occurs distally on that portion of the scale surface that is not incorporated into the seed wing (Figures 1A [left] and 2F, L–O). Abaxially the tomentose area is more extensive and occurs only on the surface that was in direct contact with the seed wings formed on the two contiguous bract–scale complexes immediately below in the cone (Figure 6L). As a result, the abaxial outline of the tomentose area (ca. 61–75 mm^2) is roughly similar to the outline of two contiguous adaxial winged seeds (Figures 1A, C [right] and 2D, E, H–K). On the distal part of the abaxial surface, cuticle preparations show the bases of abundant trichomes (Figure 4F), but whether the trichomes in this area were caducous or lost or abraded with exposure to the environment is unknown.

Individual, three-dimensionally preserved trichomes are non-glandular, distinctly conical, ca. 44–155 μm long and ca. 7–22 μm wide (Figure 4A–D). Microtome sections show that trichomes develop from a single epidermal layer (Figure 3D). Trichome bases are generally unicellular, circular to elliptical in outline, ca. 19–35 μm in diameter, with a thickened, raised margin on the outer surface of the cuticle (Figure 4D). The density of trichomes is ca. 50–80/200 μm^2.

The abaxial (outer) cuticle of the bract–scale complexes is delicate and ca. 3–4 μm thick (Figures 3D and 4B–D). On the ovuliferous scale, both proximally and also near the middle, epidermal cell outlines are approximately isodiametric, rectangular in outline, ca. 55–90 μm long and ca. 12–25 μm wide (Figure 4C, D). Distally the epidermal cells are irregularly arranged, square to polygonal in outline, and ca. 360–1700 μm^2 (Figure 4E). The abaxial cuticle of the bract shows a similar transition in the size and shape of the epidermal cell outlines (Figure 4F, G). Proximally, and also near the middle, epidermal cell outlines range from approximately isodiametric to rectangular, ca. 50–90 μm long and ca. 12–22 μm wide (Figure 4F), whereas distally, and near the margin, the epidermal cell outlines are elongated and polygonal, ca. 88–140 μm long and ca. 9–22 μm wide (Figure 4G). Small papillae are present on the abaxial side of the bract and are ca. 7–11 μm in diameter (Figure 4H).

Stomata appear randomly distributed on the abaxial surface of the ovuliferous scale but occur in a small median stomatal band on the abaxial surface of the bract. Stomatal complexes are ca. 80–110 μm long (from pole to pole of the guard cells) and ca. 50–75 μm wide (from the two outermost walls of the lateral subsidiary cells). There are two rows of complexes in the stomatal band, which is at least ~1 mm long (Figure 4I–K), and they are separated by a broad non-stomatal zone that narrows distally from ~200 μm to ~50 μm wide. The stomatal aperture is slit-like, ~10 μm long, and defined by the outlines of pairs of narrowly and rectangular to semicircular guard cells that are sunken into the epidermis. Guard cells are surrounded by a complete inner and an incomplete outer ring of subsidiary cells (Figure 4L, M). The inner ring is composed of two lateral and two polar cells, while the outer ring is composed of one or two lateral cells and one or two polar cells. Neighboring complexes in the stomatal band share polar cells (Figure 4J, K). The polar cells are roughly rectangular in outline (ca. 17–25 μm), while the inner and outer lateral cells are more or less semicircular in outline, ca. 35–55 μm long and ca. 10–18 μm wide (Figure 4L, M). The subsidiary cells are separated from the surrounding epidermal cells by two prominent cuticular flanges.

Seeds and interseminal ridge

Two winged seeds with their micropyles directed toward the cone axis (i.e., inverted) are borne proximally on the adaxial surface of each bract–scale complex (Figures 1A and 5A, B). The two seeds develop very close to each other, and together the seed bodies and wings cover approximately 78–80% of the adaxial surface of the ovuliferous scale. The two seed bodies are separated by an interseminal ridge (Figures 1B, 2G, and 5E) that does not extend more than half of the height of the seeds and is ca. 2.1–3.8 mm long and ca. 0.5–0.8 mm wide.

Seeds are ca. 9.1–11.1 mm long including the wing (n = 3, SD = 1.0), with an elliptical to ovate seed body ca. 2.5–3.2 mm long, ca. 1.2–1.8 mm wide, and ca. 50–200 μm thick (n = 10, SD = 0.3, 0.2, 0.2, respectively). The micropyle is short, ca. 115–120 μm long (Figures 1B, D [left] and 5B). Seed bodies are about one-fifth to one-sixth of the length of the ovuliferous scale and are completely or almost completely covered by wing tissue on the exposed side only (Figure 1B, D). Abscission and shedding of the seed bodies results in an ovoid, shallow cup-like depression on the adaxial surface (Figure 2B, C).

The outer cuticle of the seed is delicate, ca. 5–6 μm thick, and lacks stomata (Figure 3G, H). Epidermal cells are ca. 18–22 μm in diameter, isodiametric with mostly square, but occasionally polygonal outlines. Three tissue layers can be distinguished in transverse sections of the seeds (Figure 3G–I). The outermost tissue, the sarcotesta, is ca. 27–30 μm thick and consists of one or two layers of parenchyma cells filled with dark contents. The middle tissue, the sclerotesta, is ca. 60–110 μm thick and composed of four to six layers of polygonal, thick-walled sclerenchyma (i.e., stone cells) ca. 18–40 μm in diameter, occasionally filled

with dark contents and with characteristic simple pits (Figure 3G, H). The inner layer, the endotesta (ca. 30–45 μm thick), consists of unspecialized parenchyma cells without dark contents (Figure 3H, I).

Resin vesicles in the seed coat are not visible as raised areas on the seed coat. They are highly compressed, ca. 77–100 μm wide, and sections through the seed wall show that they occur predominantly between the sclerotesta and endotesta (Figure 3H, I).

The margin of the seed wing is curved distally and does not extend to the edge of the scale (Figure 1A, D [left]). The wing varies from ~30 μm thick near the seed body to ~20 μm thick distally and is formed by separation of the adaxial surface of the central and distal portion of the ovuliferous scale. Abscission and shedding of the wing tissue results in a conspicuous scar that exposes the smooth inner tissues of the ovuliferous scale (Figures 1C [left] and 2F, L–O).

DISCUSSION

Morphological characters supporting a relationship to Pinaceae

Four traits are important for unambiguous assignment of dispersed bract–scale complexes to Pinaceae: bracts and ovuliferous scales that are morphologically and anatomically distinct from each other, seeds that are inverted and borne on the adaxial surface of the ovuliferous scales, the consistent occurrence of two seeds per ovuliferous scale, and seeds with wings derived from the adaxial tissue of the ovuliferous scale (Rothwell et al., 2012). All of these traits can be recognized in the isolated bract–scale complexes of *Lepidocasus mellonae*, unequivocally supporting a relationship with Pinaceae. Other important features of Pinaceae seed cones, especially seed cones of the abietoids, are the presence of resin bodies in the seed coat (i.e., vesiculate seeds) and cones that disarticulate at maturity for seed dispersal (a feature of all abietoids except *Tsuga* and *Nothotsuga*).

Comparison with other Pinaceae from the Early Cretaceous of Mongolia

Lepidocasus mellonae grew together with several other species of early Pinaceae in the Tevshiin Govi flora, including two species of *Schizolepidopsis* (Leslie et al., 2013; Matsunaga et al., 2021) as well as *Picea farjonii* and *Pityostrobus stockeyae* (Herrera et al., 2016). The disarticulating mature bract–scale complexes of *L. mellonae* differ from those of *P. farjonii* and *P. stockeyae*, which are spreading/flexing cones, in being prominently ribbed and tomentose instead of smooth and glabrous (Figure 6B, C). Mature bract–scale complexes of the two *Schizolepidopsis* species differ from those of *L. mellonae* in their smooth surface (not ribbed) and deeply bilobed shape, unlike those of the new fossil (see Leslie et al., 2013).

Krassilov (1982) reported two pinaceous fossil taxa from the Early Cretaceous of Mongolia based on compression/impression specimens of isolated bract–scale complexes. *Pseudolarix erensis*, the best known, is based on associated winged seeds, leaves, and shoots (Figures 6E and 7A–G). Krassilov (1982) suggested that the cones of *P. erensis* likely disarticulated at maturity, based on the number of isolated cone scales found at the fossil localities Gurvan-Eren, Manlay, and Bon-Tsagan. The cone scales of *P. erensis* appear to show a small subtending bract and two seeds, both crucial features for the assignment of these fossils to Pinaceae (Figures 6E and 7A–G). However, the shape of the ovuliferous scales is consistently ovate with a pedicellate base. The ovuliferous scales are also rarely auricled, and lack evidence of hairs or trichome bases on the surface of the cone scales, which contrasts with the condition in *L. mellonae*. Our observations of the original material described by Krassilov (1982) suggest that the placement of *P. erensis* in Pinaceae is appropriate, but that the species is distinct from *L. mellonae* and, given the limited and not well-preserved material, assignment to the extant genus *Pseudolarix* is not secure.

The second fossil taxon from the Early Cretaceous of Mongolia, *Pityolepis* sp. (Krassilov, 1982), is based on a single ovuliferous scale and its associated bract (Figure 6D). The cone scale is obovate, ~20 mm long and ~14 mm wide at the broadest part. Krassilov described the bracts as obcuneate, awned, and flabellately striated, based on detached bract-like structures found in association with the single ovuliferous scale. The size and obovate shape of the ovuliferous scale, and its ribbed surface, are similar to that seen in *L. mellonae*, but the associated awned bract-like structures are very different. It is also unclear whether the adaxial and abaxial surfaces of *Pityolepis* sp. were tomentose. We are therefore reluctant to assign Krassilov's specimens to *L. mellonae*.

Comparison with cone scales of other Mesozoic Pinaceae

The bract–scale complexes of *Lepidocasus mellonae* are similar to the isolated cone scales of several species assigned to the morphogenus *Pityolepis* based on compression/impression specimens from Middle Jurassic to Early Cretaceous localities in Laurasia (Figures 6F–K and 7H, I). The consistent occurrence of disarticulated *Pityolepis* bract–scale complexes for these species implies shedding dispersal and, combined with clear morphological similarities to *L. mellonae*, suggests that all these fossils belong to the same group of pinaceous plants. However, this hypothesis is difficult to test without more detailed information.

Pityolepis was first mentioned by Nathorst (1897) as an informal subdivision within the genus *Pinites* when he described isolated bract–scale complexes as *Pinites* (*Pityolepis*) *tsugaeformis* and *Pinites* (*Pityolepis*) *pygmaeus* from Hanaskogdalen (Svalbard, Norway) (Figures 6G, H and 7H, I). These fossils were first regarded as of Jurassic age, but are now considered of Early Cretaceous (Aptian–Albian) age

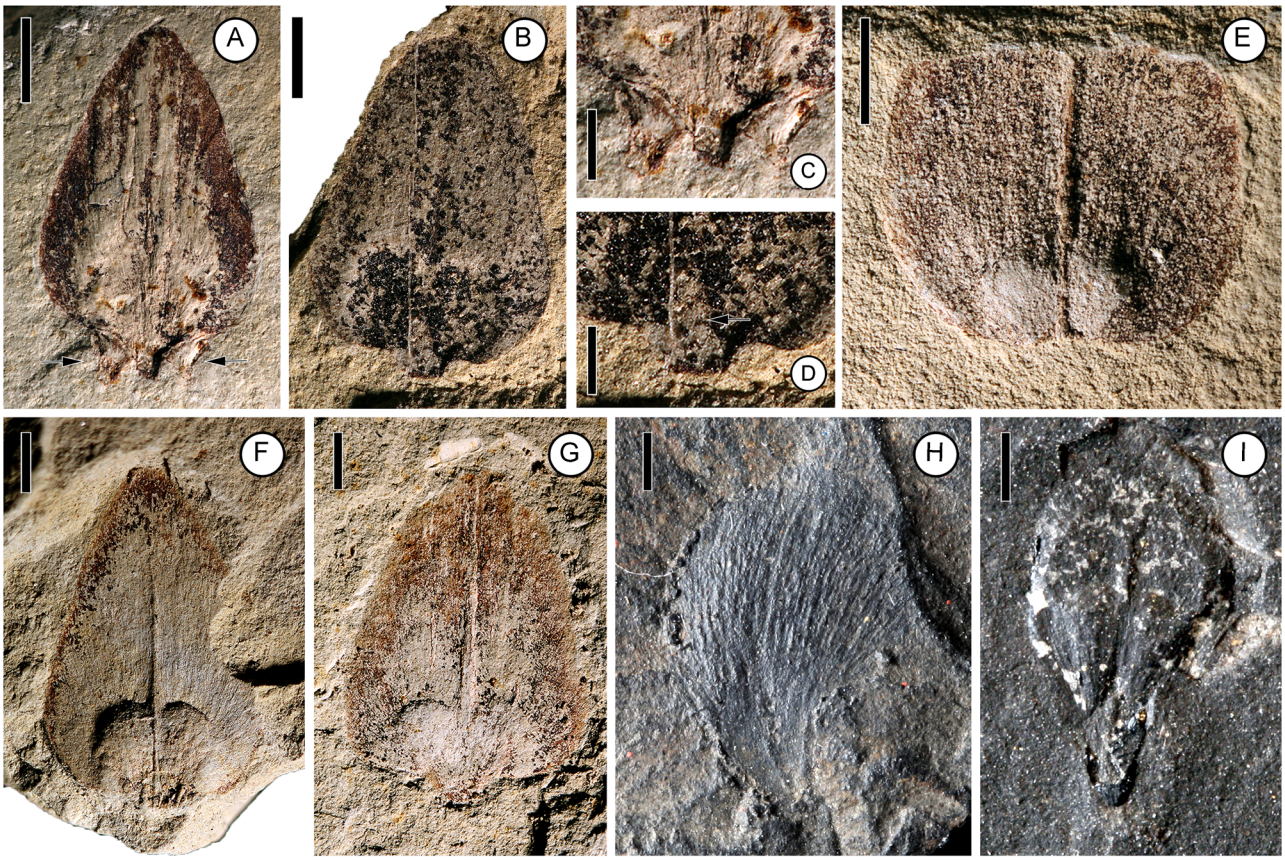

FIGURE 7 Selected fossil bract–scale complexes from the Early Cretaceous. (A–G) *Pseudolarix erensis* from Mongolia (Krassilov, 1982). (A) Holotype; presumed abaxial view showing auricles (arrows) (N3149/3001). (B) Abaxial view (N3149/3290). (C) Detail from A, showing auricles. (D) Detail from B, showing the poorly preserved bract. (E) Adaxial view of small broad bract–scale complex showing the conspicuous central furrow and impressions of the cups formed by the two seed bodies (N3149/3291). (F, G) Adaxial views showing the conspicuous central furrow and impressions of the cups formed by the two seed bodies (N3149/3298, 3285). (H, I) *Pinites* (*Pityolepis*) *tsugaeformis* and *Pinites* (*Pityolepis*) *pygmaeus* from Svalbard (Nathorst, 1897) (S092633, S020672). Scale bars = 2 mm (A, B, E–K); 1 mm (C, D)

(see review in Pott, 2014). The specimens are not well preserved and appear to show cone scales that are obovate in shape and ribbed, bearing two seeds.

The genus name *Pityolepis* Nathorst was established by Nathorst (1907) with the description of the species *P. tollii* Nathorst (type species) from the Arctic of Russia (Kotel'nyi Island) (Figure 6F [right]). Like the Hanaskogdalen specimens, this fossil material was treated originally as Jurassic, but radiometric dating indicates an Albian age (see Herman and Spicer, 2010). Unfortunately, the original Nathorst (1907) collection, which included associated abundant dispersed *Pityospermum* winged seeds and shed *Pityophyllum* leaves, appears to have been lost (A. B. Herman, personal communication), but Nathorst's (1907) original description, as well as specimens identified as *P. tollii* (Figure 6F [left]) collected more recently from Kotel'nyi Island (Herman and Spicer, 2010), indicate that *P. tollii* had unusual large bract–scale complexes (ca. 6–9 cm long) that vary from elliptical with an elongated apex to concave-convex to obovate with two seeds. Independent of variation in the cone scale shape and size, all of the specimens of *P. tollii* are characterized by a strongly ribbed surface, very similar to the abaxial and adaxial surfaces of *L. mellonae* (Figures 1 and 2). Other *Pityolepis* species, such as *P. sphenoides* (Figure 6J) from the Middle to Late Jurassic of China (Zheng et al., 2001) and *P. rugosa* (Figure 6I) from the Early Cretaceous (?) of Greenland (Seward, 1927), are also characterized by strongly ribbed surfaces. Only *P. crassa* (Figure 6K) from the Early Cretaceous of Russia (Prynada, 1962) appears to have both a ribbed and conspicuously tomentose surface as seen in *L. mellonae* (Figures 1 and 2).

A large number of *Pityostrobus* species have been described based on fossil cones from Early Cretaceous localities, but none shows any indication of a shedder dispersal (e.g., Herrera et al., 2016; Smith et al., 2016; Gernandt et al., 2018; Losada et al., 2018). Most have also been described on the basis of permineralized material, which can be challenging to compare with the abundant lignified specimens on which *L. mellonae* is based. Nevertheless, a few *Pityostrobus* species have trichomes on different parts of the seed cones that are comparable to those present in *L. mellonae*. Trichomes or trichome–like structures have been reported from Aptian and/or Albian species

such as *P. milleri* (Falder et al., 1998), *P. hokodzensis* (Ratzel et al., 2001), *P. hueberi* (Robison and Miller, 1977), *P. ramentosa* (Miller, 1976), *P. virginiana* (Robison and Miller, 1977), and *P. pluriresinosa* (Smith et al., 2016), as well as two species from the Late Cretaceous: *P. pubescens* (Miller, 1985) and *P. beardii* (Smith and Stockey, 2002). Information on the distribution of the tomentose layer in the permineralized fossils is limited; nonetheless, in all cases, trichomes appear elongate and unicellular as in *L. mellonae*. However, none of the above *Pityostrobus* species appears to have densely spaced trichomes on both the abaxial and adaxial surfaces of the ovuliferous scales.

Based on our comparisons of the isolated bract–scale complexes of *Pityolepis* species and articulated seed cones of *Pityostrobus* species that have been described from Cretaceous localities in the Northern Hemisphere, we consider that the designation of the new genus *Lepidocasus* is most appropriate for the Tevshiin Govi fossil material, which is well characterized and has an unequivocal "shedder" dispersal syndrome.

Comparison with extant Pinaceae

Lepidocasus mellonae differs from all extant genera of the pinoid clade (i.e., *Pinus*, *Picea*, *Pseudotsuga*, *Larix*, and *Cathaya*) as well as from two abietoid genera (*Nothotsuga*, *Tsuga*) that have cones with persistent flexing/spreading cone scales. The remaining abietoid genera (*Abies*, *Cedrus*, *Keteleeria*, and *Pseudolarix*) are shedders, but none has bract–scale complexes similar in morphology and anatomy to *L. mellonae*. Bract–scale complexes of *Abies* are broad-flabellate with conspicuous auricles, and the bract is usually exerted and recurved (Figure 5G–L). Bract–scale complexes of *Cedrus* are also broadly flabellate, but with a median notch and a pedicellate base (Figure 8F). Bract–scale complexes of *Keteleeria* are elliptic to ovoid in outline but usually with leafy bracts that are exerted rather than obovate and non-exerted (Figure 5M–R). Bract–scale complexes of *Pseudolarix* (Figure 8A) are ovate, usually with a sharp acute/acuminate apex and a pedicellate base, and the bract is tridentate.

Despite the morphological differences between *L. mellonae* and the four abietoid genera with shedding seed cones, there are several anatomical similarities between *L. mellonae* and the cones of these genera. For example, their seeds have resin bodies in the seed coat (vesiculate), and their mature ovuliferous scales are strongly longitudinally ribbed, which results from a combination of abundant resin canals and vascular strands in the tissues of the seed scale (Figure 5A, F, H, J, L–O). *Lepidocasus mellonae* and the extant genera *Abies* and *Tsuga* also share an initial medial separation of the bract from the ovuliferous scale (Figure 5C, J). The small stomatal band present on the abaxial side of the bract and the seemingly random stomata on the ovuliferous scale (Figure 4I–M) are also similar to the stomata seen in leaves of *Abies* and *Cedrus*, and also *Picea* (pinoid) (Miranda and Chaphekar, 1980; Napp–Zinn and Hu, 1989; Herting, 2017). A recent review of leaf anatomy in all genera of living Pinaceae shows that *Abies*, *Cedrus*, and *Picea* possess up to eight subsidiary cells that are arranged in two rings around the guard cells (i.e., "*Abies*-type" of Herting, 2017) as also in *L. mellonae* (Figure 4I–M). Unfortunately, the leaves of *L. mellonae* have not yet been recognized, and little is known about how stomata on the bract–scale complexes of living Pinaceae might differ from those of the leaves. Nevertheless, stomatal anatomy in *L. mellonae* suggests that more detailed information, ideally from leaves associated with the new fossil, could be helpful in providing more insight into potential relationships with genera of extant abietoids.

Another connection between *L. mellonae* and abietoids such as *Cedrus* and *Pseudolarix* is the well-developed indumentum on the bract–scale complexes. In *L. mellonae* this covers the entire abaxial side of the ovuliferous scale as well as the distal portion of the adaxial surface, whereas the cones of all other Pinaceae at Tevshiin Govi are glabrous and lack trichome bases in their cuticles (Leslie et al., 2013; Herrera et al., 2016). In *L. mellonae*, as also in *Cedrus* and *Pseudolarix*, the tomentose surface of the cone scale appears to be defined by the shape of the winged seeds (Figures 6L and 8). Abaxially the extent of tomentum is influenced by the winged seeds borne on the ovuliferous scales directly above (Figures 1, 2, 4A–E, and 8). Adaxially, the extent of tomentum is restricted to the distal intact epidermal surface that is not incorporated into the wing (Figures 1, 2, and 8).

All the bract–scale complexes of shedding cones of extant Pinaceae that we have observed have a dense tomentum on the abaxial side (Figure 8). However, while the trichomes of *L. mellonae* appear non-glandular based on their conical shape and acute tip (Figures 3D and 4A–D), trichomes of living *Pseudolarix* and *Cedrus* have rounded apices (Figure 8; see also Hu et al., 1989). Observations from an extant *Picea* hybrid (pinoid) document the presence of glandular and non-glandular trichomes on young stems (Celedon et al., 2020). Additional work is needed to evaluate the form, function(s), and systematic utility of trichomes in Pinaceae, as well as their occurrence on different plant parts (cone axes, leaves, shoots, etc.). In general, the role and evolution of plant trichomes in gymnosperms, and especially in conifers, has received relatively little attention and deserves more detailed study (Hu et al., 1989; Celedon et al., 2020).

Phylogenetic placement of *Lepidocasus mellonae*

Parsimony analysis of the phylogenetic position of *L. mellonae* and other living and fossil Pinaceae yielded a single most parsimonious tree of 22,003 steps (consistency index: 0.693, retention index: 0.777, rescaled consistency index: 0.539) (Figure 9; Appendix S4). This result is similar to the reduced consensus tree based on parsimony of the combined morphology and plastid DNA data set obtained by Gernandt et al. (2018), including the placement of the early pinaceous seed cone *Eathiestrobus mackenziei* from the Late Jurassic (Rothwell et al., 2012) as sister to the abietoids and

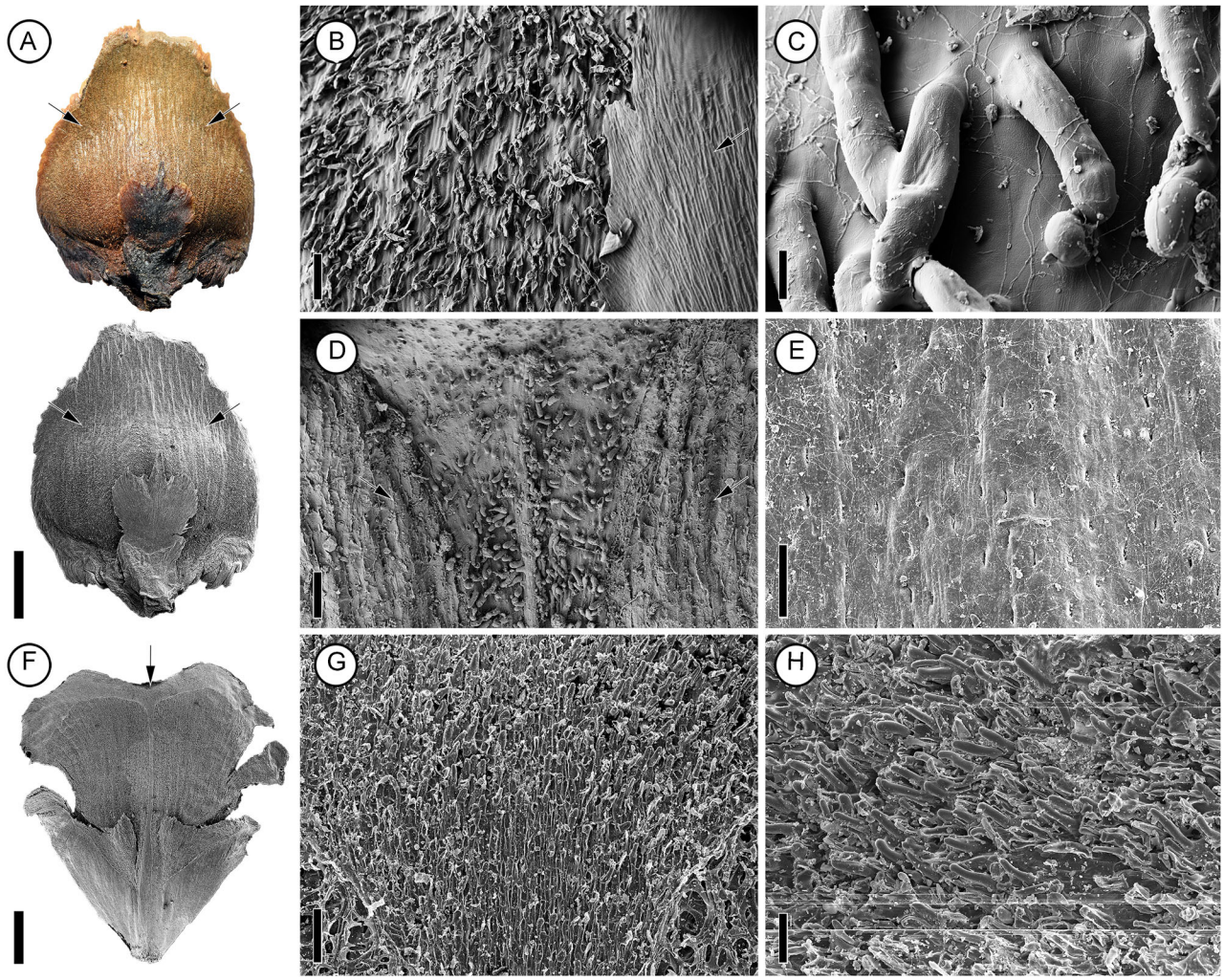

FIGURE 8 Bract–scale complexes of extant Pinaceae: light (A, top) and scanning electron (A, bottom; B–H) micrographs. (A–E) *Pseudolarix amabilis* (Nelson) Rehder. (A) Abaxial view of mature bract–scale complex showing the bract and the upper limit of trichomes (arrows). (B) Detail of abaxial view showing the glabrous surface of the bract (arrow) and the tomentose surface of the ovuliferous scale. (C) Detail of abaxial surface of the ovuliferous scale showing unicellular trichomes. (D) Detail of adaxial surface of the ovuliferous scale showing distal tomentose area between the area from which both winged seeds have been shed (arrows). (E) Detail of abaxial view of bract showing stomata. (F–H) Extant *Cedrus deodara* (Roxb. ex D.Don) G.Don. (F) Adaxial view of mature bract–scale complex showing the bract, seed scars, and tomentose distal area (arrow). (G) Detail from F showing tomentose distal area. (H) Detail of unicellular trichomes from abaxial surface of ovuliferous scale. Scale bars = 5 mm (A, F); 200 μm (B, D, E, G); 100 μm (H); 20 μm (C)

pinoids (see Gernandt et al., 2018: Figure 5E). However, contrary to Gernandt et al. (2018), the fossil genus *Obirastrobus* is placed within pinoids (Appendix S4). *Lepidocasus mellonae* is placed as sister to extant *Cedrus deodara* and both are sister to the remaining abietoids and pinoids (Figure 9). Bootstrap support is low (55%) and *L. mellonae* and *C. deodara* are mainly united by the presence of similar anatomical features at the base of the ovuliferous cones in shedder cones (morphological character 189) (see also Losada et al., 2018). The leaves, shoots, and pollen cones of *L. mellonae* are still unknown, and it is possible that its position within Pinaceae will change as more data become available. Nevertheless, a broad affinity to *Abies*, *Cedrus*, *Keteleeria*, and *Pseudolarix*, the four extant abietoid genera with shedding seed cones, is clear and is also supported by the presence of vesiculate seeds.

Dispersal syndrome of *Lepidocasus mellonae* and the evolution of scale shedding in Pinaceae

Lepidocasus mellonae grew together with at least four other species of Pinaceae in the Tevshiin Govi swamp, making pinaceous conifers the most diverse component of the paleoflora (Leslie et al., 2013; Herrera et al., 2016; Matsunaga et al., 2021). The remarkable abundance of pinaceous fossils in the lignite also suggests that the local vegetation was dominated by this group of conifers. However, *L. mellonae* occurs in only two of the 111 samples that have been processed from Tevshiin Govi and therefore appears to have been relatively rare on the landscape.

In contrast to the abundance of cone scales of *L. mellonae*, hundreds of articulated seed cones of other fossil Pinaceae have been recovered from the Tevshiin Govi

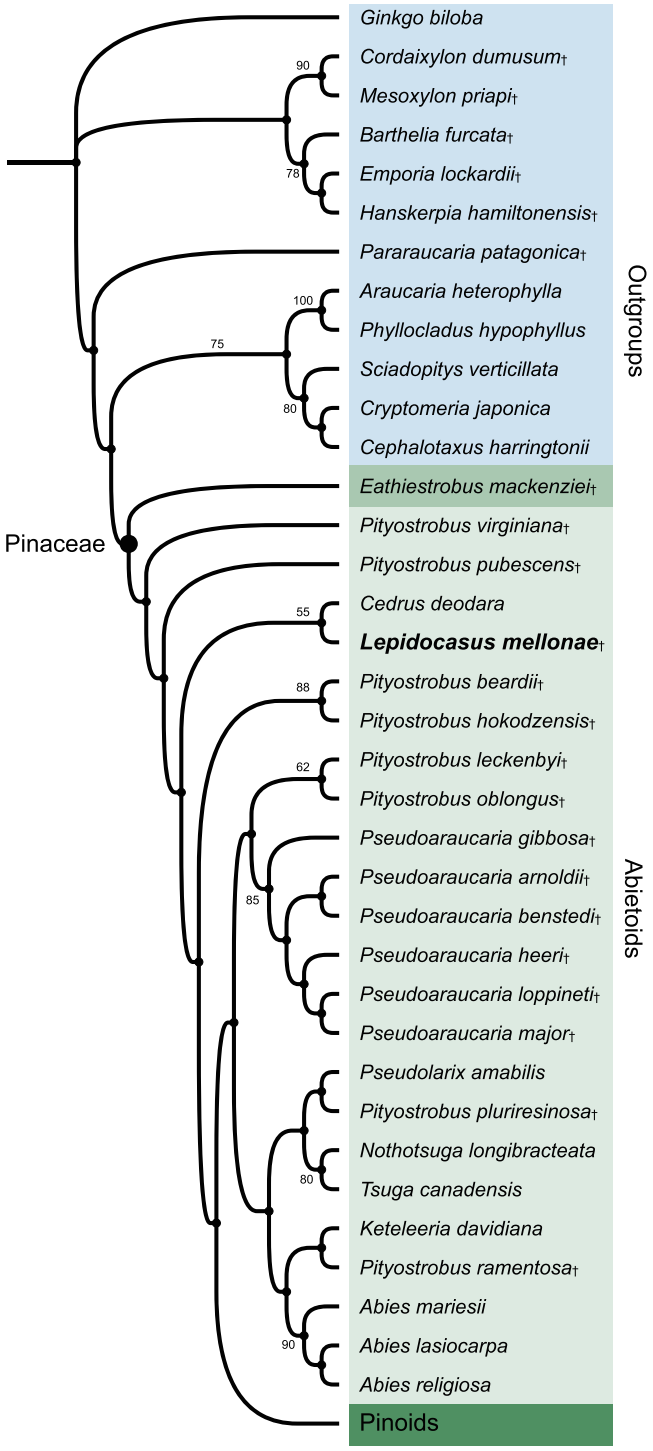

FIGURE 9 Phylogenetic analysis of living and fossil Pinaceae based on combined morphology and plastid DNA (see also Gernandt et al., 2018). The analysis yielded one most parsimonious tree (for complete tree, see Appendix S4). *Lepidocasus mellonae* is placed as sister to extant *Cedrus deodara* and both are sister to the remaining members of the family. Bootstrap values given for nodes >50%. Fossil taxa are indicated with †

fossil assemblage, including cones of *Picea farjonii* (>100 specimens) and *Pityostrobus stockeyae* (>600 specimens) (Herrera et al., 2016). Seed cones of two fossil Cupressaceae, *Pentakonos diminutus* (>50 specimens) and *Stutzeliastrobus foliatus* (>200 specimens), are also common among the Tevshiin Govi samples (Herrera et al., 2017). However, for *L. mellonae* the only evidence of attachment is one cone scale attached to a fragmentary axis (Figure 1C). The large number of disarticulated specimens recovered from the lignite strongly implies that the cone scales of *L. mellonae* were regularly shed for seed dispersal and that the separation is not a result of sample preparation or taphonomy. Similarly, only two specimens have been recovered with seeds still attached to the adaxial surface of the ovuliferous scale (Figure 1A, B, D), making it clear that shedding of the seeds from the scales was also a consistent feature of the dispersal for this plant.

The anatomical details observed from the bract–scale complexes of *L. mellonae* also provide additional evidence of its shedder dispersal syndrome. Transverse sections near the base of the cone scale show a lack of prominent xylem composed of relatively few tracheids with broad lumens, which are surrounded by a large sclerenchymatous zone (Figure 3A, B). This is consistent with a precise mode of preprogrammed disarticulation, as observed in the "shedder" cones of extant abietoids (Losada et al., 2018), and is especially similar to the situation in extant *Cedrus* (Losada et al., 2018). Shedding of cone scales and seeds is not unique at Tevshiin Govi. It has also been reconstructed for *Krassilovia mongolica*, an extinct conifer that grew together with *L. mellonae*. The shedder dispersal syndrome of *K. mongolica* is also based on the recovery of several thousands of disarticulated seed cone scales and anatomical features (Herrera et al., 2015, 2020).

The recognition of *L. mellonae* as a shedding seed cone from the Aptian–Albian of Mongolia is especially relevant for understanding the early evolutionary history of Pinaceae. Although a shedding dispersal syndrome has been inferred from other potential pinaceous taxa of Jurassic and Early Cretaceous age (e.g., Nathorst, 1907; Krassilov, 1982; Zheng et al., 2001), distinguishing of *L. mellonae* as a shedder raises the question of whether other shedding taxa have been overlooked in phylogenetic and other discussions of Pinaceae evolution (e.g., Stockey, 1981; Miller, 1988; Taylor et al., 2009; Smith et al., 2016; Gernandt et al., 2018) that lean heavily on permineralized specimens. Assessing the systematic affinities of isolated cone scales (sometimes associated with leaves and winged seeds) can be difficult in the absence of anatomical data, but a reevaluation of such material, especially of specimens of unequivocal Jurassic age or older (e.g., Zheng et al., 2001; Domogatskaya and Herman, 2019), could be important to understand the early history of seed dispersal in the family and perhaps also to reconcile the gap between the fossil record and molecular age estimates for the family based on extant Pinaceae.

ACKNOWLEDGMENTS

The authors thank T. Gombosuren, L. Uranbileg, and K. Matsunaga for assistance with fieldwork in Mongolia; M. Von Konrat and the Grainger Bioinformatics Center (GBC; Field Museum) for digital imaging; A. I. Neander for aid with X-ray

tomography; C. Dong for SEM scanning of living Pinaceae; G. Bedoya for nomenclatural suggestions; E. Bugdaeva, N. Nosova, C. Pott, O. Johansson, and A. B. Herman for photographs of related fossils; D. S. Gernandt for providing information regarding the morphological matrix; J. Herting and J. M. Losada for comments regarding the anatomy of extant Pinaceae; and A. A. Klymiuk for data curation. F. H. thanks B. Himschoot for constant support. We also thank the reviewers for their helpful comments and suggestions. Funding for this work was provided by the National Science Foundation grants DEB-1748286 (to P.S.H., P.R.C., and F.H.), DEB-1348456 (to P.S.H. and P.R.C.), and the Oak Spring Garden Foundation (to F.H.).

AUTHOR CONTRIBUTIONS

F.H. led conception and design of the project with P.S.H. and P.R.C. F.H., P.S.H., and P.R.C. provided funding for the project. F.H., G.S., M.A.B., N.I., A.B.L., P.R.C., and P.S.H. participated in fieldwork, sample processing, and analyses and visualization of data. F.H. wrote the initial manuscript draft; all authors reviewed and edited further drafts.

OPEN RESEARCH BADGES

This article has been awarded Open Materials and Open Data badges. All materials and data are publicly accessible via the Open Science Framework at http://morphobank.org/permalink/?P3725 and https://doi.org/10.5061/dryad.2z34tmpkc. Learn more about the Open Practices badges from the Center for Open Science: https://osf.io/tvyxz/wiki

DATA AVAILABILITY STATEMENT

Fossil material is housed in the paleobotanical collections of the Field Museum, Chicago, Illinois (FMNH: collection numbers with the prefix PP) and in the Institute of Paleontology in Ulaanbaatar, Mongolia (Mongolian Paleontological Center–Flora); see Systematics for accession numbers. The morphological data matrix is available on MorphoBank (http://morphobank.org/permalink/?P3725).

ORCID

Fabiany Herrera http://orcid.org/0000-0002-2412-672X
Gongle Shi https://orcid.org/0000-0003-3374-6637
Maya A. Bickner https://orcid.org/0000-0002-1974-5593
Niiden Ichinnorov https://orcid.org/0000-0001-9044-5940
Andrew B. Leslie https://orcid.org/0000-0002-9011-6888
Peter R. Crane https://orcid.org/0000-0003-4331-6948
Patrick S. Herendeen http://orcid.org/0000-0003-2657-8671

REFERENCES

Alvin, K. L. 1957a. On the two cones *Pseudoaraucaria* heeri (Coemans) nov. comb. and *Pityostrobus villerotensis* nov. sp. from the Wealden of Belgium. *Institut Royal des Sciences Naturelles de Belgique Memoires* 135: 1–27.

Alvin, K. L. 1957b. On *Pseudoaraucaria* Fliche emend., a genus of fossil pinaceous cones. *Annals of Botany* 21: 33–51.

Alvin, K. L. 1960. Further conifers of the Pinaceae from the Wealden Formation of Belgium. *Institut Royal des Sciences Naturelles de Belgique Memoires* 146: 1–39.

Alvin, K. L. 1988. On a new specimen of *Pseudoaraucaria* major Fliche (Pinaceae) from the Cretaceous Isle of Wight. *Botanical Journal of the Linnean Society* 97: 159–170.

Celedon, J. M., J. G. A. Whitehill, L. L. Madilao, and J. Bohlmann. 2020. Gymnosperm glandular trichomes: expanded dimensions of the conifer terpenoid defense system. *Scientific Reports* 10: 12464.

Domogatskaya, K.V. and A. B. Herman. 2019. New species of the genus *Schizolepidopsis* (conifers) from the Albian of the Russian high Arctic and geological history of the genus. *Cretaceous Research* 97: 73–93.

Falder, A. B., G. W. Rothwell., G. Mapes., R. H. Mapes., and L. A. Doguzhaeva. 1998. *Pityostrobus milleri* sp. nov., a pinaceous cone from the Lower Cretaceous (Aptian) of southwestern Russia. *Review of Palaeobotany and Palynology* 103: 253–261.

Farjon, A. 2010. A handbook of the world's conifers. Brill, Leiden, The Netherlands.

Gernandt, D. S., C. Reséndiz Arias, T. Terrazas, X. Aguirre Dugua, and A. Willyard. 2018. Incorporating fossils into the Pinaceae tree of life. *American Journal of Botany* 105: 1329–1344.

Graham, S. A., M. S. Hendrix, C. L. Johnson, D. Badamgarav, G. Badarch, J. Amory, M. Porter, et al. 2001. Sedimentary record and tectonic implications of Mesozoic rifting in southeast Mongolia. *Geological Society of America Bulletin* 113: 1560–1579.

Hasegawa, H., H. Ando, N. Hasebe, N. Ichinnorov, T. Ohta, T. Hasegawa, M. Yamamoto, et al. 2018. Depositional ages and characteristics of Middle–Upper Jurassic and Lower Cretaceous lacustrine deposits in southeastern Mongolia. *Island Arc* e12243: 1–17.

Herman, A. B., and R. A. Spicer. 2010. Mid-Cretaceous floras and climate of the Russian high Arctic (Novosibirsk Islands, Northern Yakutiya). *Palaeogeography, Palaeoclimatology, Palaeoecology* 295: 409–422.

Herrera, F., A. B. Leslie, G. Shi, P. Knopf, N. Ichinnorov, M. Takahashi, P. R. Crane, and P. S. Herendeen. 2016. New fossil Pinaceae from the Early Cretaceous of Mongolia. *Botany* 94: 885–915.

Herrera, F., G. Shi, P. Knopf, A. B. Leslie, N. Ichinnorov, M. Takahashi, P. R. Crane, and P. S. Herendeen. 2017. Cupressaceae conifers from the Early Cretaceous of Mongolia. *International Journal of Plant Sciences* 178: 19–41.

Herrera, F., G. Shi, A. B. Leslie, P. Knopf, N. Ichinnorov, M. Takahashi, P. R. Crane, and P. S. Herendeen. 2015. A new voltzian seed cone from the Early Cretaceous of Mongolia and its implications for the evolution of ancient conifers. *International Journal of Plant Sciences* 176: 791–809.

Herrera, F., G. Shi, C. Mays, N. Ichinnorov, M. Takahashi, J. J. Bevitt, P. S. Herendeen, and P. R. Crane. 2020. Reconstructing *Krassilovia mongolica* supports recognition of a new and unusual group of Mesozoic conifers. *PLoS One* 15e0226779: 1–21.

Herting, J. 2017. Biodiversity of extant and fossil Cupressaceae s.l. and Pinaceae from the Lower Cretaceous of Mongolia. Ph.D. dissertation, Ruhr-Universität Bochum, Bochum, Germany.

Hu, Y., K. Napp–Zinn, and D. Winne. 1989. Comparative anatomy of seed–scales of female cones of Pinaceae. *Botanische Jahrbücher fur Systematik, Pflanzengeschichte und Pflanzengeographie* 111: 63–85.

Ichinnorov, N. 2003. Palynocomplex of the Lower Cretaceous sediments of Eastern Mongolia. *Mongolian Geoscientist* 22: 12–16.

Ichinnorov, N., L. Jargal, N. Odgerel, and A. Enkhtuya. 2012. Palynology and petrology characteristics of the Lower Cretaceous Tevshiin Gobi coal deposit, Mongolia. 11th Symposium on Mesozoic Terrestrial Ecosystems. August 15–18, Korea.

Krassilov, V. A. 1982. Early Cretaceous flora of Mongolia. *Palaeontographica B* 181: 1–43.

Leslie, A. B., J. Beaulieu, G. Holman, C. S. Campbell, W. Mei, L. R. Raubeson, and S. Mathews. 2018. An overview of extant conifer evolution from the perspective of the fossil record. *American Journal of Botany* 105: 1531–1544.

Leslie, A. B., J. M. Beaulieu, H. S. Rai, P. R. Crane, M. J. Donoghue, and S. Mathews. 2012. Hemisphere–scale differences in conifer evolutionary dynamics. *Proceedings of the National Academy of Sciences USA* 109: 16217–16221.

Leslie, A. B., I. Glasspool, P. S. Herendeen, N. Ichinnorov, P. Knopf, M. Takahashi, and P. R. Crane. 2013. Pinaceae-like reproductive morphology in *Schizolepidopsis canicularis* sp. nov. from the Early Cretaceous (Aptian–Albian) of Mongolia. *American Journal of Botany* 100: 2426–2436.

Losada, J. M., N. Blanco-Moure, and A. B. Leslie. 2018. Not all 'pine cones' flex: functional trade-offs and the evolution of seed release mechanisms. *New Phytologist* 222: 396–407.

Matsunaga, K. K. S., P. S. Herendeen, F. Herrera, N. Ichinnorov, P. R. Crane, and G. Shi. 2021. Ovulate cones of *Schizolepidopsis ediae* sp. nov. provide insights into the evolution of Pinaceae. *International Journal of Plant Sciences* 182: 490–507.

Miller, C. N., Jr. 1976. Two new pinaceous cones from the Early Cretaceous of California. *Journal of Paleontology* 50: 821–832.

Miller, C. N., Jr. 1985. Pityostrobus pubescens, a new species of pinaceous cones from the Late Cretaceous of New Jersey. *American Journal of Botany* 72: 520–529.

Miller, C. N., Jr. 1988. The origin of modern conifer families. In C. B. Beck [ed.], Origin and evolution of gymnosperms, 448–486. Columbia University Press, New York.

Miller, C. N., Jr., and C. R. Robison 1975. Two new species of structurally preserved pinaceous cones from the Late Cretaceous of Martha's Vineyard Island, Massachusetts. *Journal of Paleontology* 49: 138–150.

Miranda, V., and M. F. L. S. Chaphekar. 1980. SEM study of the inner periclinal surface of leaf cuticles in the family Pinaceae. *Botanical Journal of the Linnean Society* 81: 61–78.

Napp–Zinn, K., and Y. Hu. 1989. Anatomical studies on the bracts in pinaceous female cones III. Comparative study of (mostly Chinese) representatives of all genera. Botanische Jahrbücher fur Systematik, *Pflanzengeschichte und Pflanzengeographie* 110: 461–477.

Nathorst, A. G. 1897. Zur mesozoischen Flora Spitzbergens. *Kongliga Svenska Vetenskaps-Akademiens Handlingar* 30: 1–77.

Nathorst, A. G. 1907. Über Trias-und Jurapflanzen von der Insel Kotelny. *Memoirs of the Academy of Imperial Science St.-Petersburg VIII ser*. XXI: 1–13.

Nichols, D. J., M. Matsukawa, and M. Ito. 2006. Palynology and age of some Cretaceous nonmarine deposits in Mongolia and China. *Cretaceous Research* 27: 241–251.

Ohsawa, M. N., and H. Nishida. 1992. Structure and affinities of the petrified plants from the Cretaceous of northern Japan and Saghalien. XII. *Obirastrobus* gen. nov., petrified pinaceous cones from the Upper Cretaceous of Hokkaido. *Journal of Plant Research* 105: 461–484.

Pott, C. 2014. The Upper Triassic flora of Svalbard. *Acta Palaeontologica Polonica* 59: 709–740.

Prynada, V. D. 1962. Mezozoyskaya flora Vostochnoy Sibiri i Zabaykal'ya. Gosgeoltekhizdat, Moscow (Mesozoic flora of the East Siberia and Transbaikalia, in Russian).

Ran, J.–H., T.–T. Shena, H. Wua, X. Gongb, and X.–Q. Wanga. 2018. Phylogeny and evolutionary history of Pinaceae updated by transcriptomic analysis. *Molecular Phylogenetics and Evolution* 129: 106–116.

Ratzel, S. R., G. W. Rothwell., G. Mapes., R. H. Mapes., and L. A. Doguzhaeva. 2001. Pityostrobus hokodzensis, a new species of pinaceous cone from the Cretaceous of Russia. *Journal of Paleontology* 75: 895–900.

Robison, C. R., and C. N. Miller, Jr. 1977. Anatomically preserved seed cones of the Pinaceae from the Early Cretaceous of Virginia. *American Journal of Botany* 64: 770–779.

Rothwell, G. W., G. Mapes, R. A. Stockey, and J. Hilton. 2012. The seed cone *Eathiestrobus* gen. nov.: Fossil evidence for a Jurassic origin of Pinaceae. *American Journal of Botany* 99: 708–720.

Seward, A. C. 1919. Fossil Plants, Volume IV. Ginkgoales, Coniferales, Gnetales. Cambridge University Press, Cambridge.

Seward, A. C. 1927. The Cretaceous Plant–Bearing Rocks of Western Greenland. *Philosophical Transactions of the Royal Society of London. Series B, Containing Papers of a Biological Character* 215: 57–175.

Shi, G., A. B. Leslie, P. S. Herendeen, F. Herrera, N. Ichinnorov, M. Takahashi, P. Knopf, and P. R. Crane. 2016. Early Cretaceous *Umkomasia* from Mongolia: implications for homology of corystosperm cupules. *New Phytologist* 210: 1418–1429.

Smith, S. Y., and R. A. Stockey. 2002. Permineralized pine cones from the Cretaceous of Vancouver Island, British Columbia. *International Journal of Plant Sciences* 163: 185–196.

Smith, S. Y., R. A. Stockey, G. W. Rothwell, and S. A. Little. 2016. A new species of *Pityostrobus* (Pinaceae) from the Cretaceous of California: Moving towards understanding the Cretaceous radiation of Pinaceae. *Journal of Systematic Palaeontology* 15: 69–81.

Stockey, R. A. 1981. Some comments on the origin and evolution of conifers. *Canadian Journal of Botany* 59: 1932–1940.

Swofford, D. L. 2003. PAUP*: Phylogenetic analysis using parsimony (*and other methods), version 4.0a. Sinauer, Sunderland, Massachusetts, USA.

Taylor, T. N., E. L. Taylor, and M. Krings. 2009. Paleobotany: The biology and evolution of fossil plants, 2nd ed. Academic Press, Burlington, Massachusetts, USA.

Zhang, J., A. D'rozario, Y. Jianxian, W. Zhenjie, and L. Wang. 2011. A new species of the extinct genus *Schizolepis* from the Jurassic Daohugou flora, Inner Mongolia, China with special reference to the fossil diversity of evolutionary implications. *Acta Geologica Sinica* 85: 471–481.

Zheng, S.-L., W. Zhang, and Q.-H. Ding. 2001. Discovery of fossil plants from Middle–Upper Jurassic Tuchengzi Formation in Western Liaoning, *China. Acta Palaeontologica Sinica* 40: 67–85.

SUPPORTING INFORMATION

Additional supporting information may be found online in the Supporting Information tab for this article.

APPENDIX S1. Video of CT data set from *Lepidocasus mellonae* (holotype PP60450) in longitudinal digital section.
APPENDIX S2. Video of CT data set from *Lepidocasus mellonae* (holotype PP60450) in transverse digital section.
APPENDIX S3. Video of translucent volume rendering from *Lepidocasus mellonae* (holotype PP60450).
APPENDIX S4. Complete most parsimonious tree of phylogenetic analysis of living and fossil Pinaceae based on combined morphology and plastid DNA.

How to cite this article: Herrera, F., G, Shi, M. A. Bickner, N. Ichinnorov, A. B. Leslie, P. R. Crane, and P. S. Herendeen. 2021. Early Cretaceous abietoid Pinaceae from Mongolia and the history of seed scale shedding. *American Journal of Botany*. 108(8): 1483–1499. https://doi.org/10.1002/ajb2.1713